Investigating the deformation timing and kinematics of the mylonitic shear zone in the North American Cordilleran metamorphic core complexes

Terry Lee[1] (terrywaihol@unr.edu), **Tatiana A. Sihpo**[2], **Andrew V. Zuza**[1], **Margaret L. Odlum**[2]

[1]Nevada Bureau of Mines and Geology, Nevada Geosciences, University of Nevada, Reno

[2]Scripps Institution of Oceanography, University of California, San Diego

NEVADA GEOSCIENCES University of Nevada, Reno · nbmg · UC San Diego SCRIPPS INSTITUTION OF OCEANOGRAPHY

Session: T162
Poster Booth No.: 222

Supported by the GSA Graduate Student Research Grant

Key qestions

(1) What are the deformation age distributions across the mylonite zone into the infrastructure?

(2) Are the mylonitic fabrics temporally decoupled from regional extension and detachment faulting?

(3) Does the infrastructure record mid-crustal deformation during Mesozoic contractional tectonics?

(4) Can apatite U-Pb petrochronology coupled with CVA analysis provide direct constraints on ductile deformation ages?

Introduction

North American Cordilleran metemorphic core complexes (MCCs) expose metamorphosed infrastructure (lower plate) which is juxtaposed against the brittlely deformed suprastructure (upper plate). These two structural domains are seperated by a high-strain mylonitic shear zone. The evolution of mylonitic shear zones is highly debated. In addition, Mesozoic-Cenozoic inherited sturctures within the infrastructure may also affect the architecture of MCCs in the North American Cordillera.

Here, we apply detailed field observations and apatite U-Pb petrochronology coupled with EBSD mircostructure to directly constrain the timing, kinematics, and conditions of ductile deformation within the mylonitic shear zone and migmatitic infrastructure. We applied this approach to Ruby Mountains-East Humboldt Range (REHR), Chemehuevi, and Catalina-Rincon MCCs, which in turn, places age constraints on the Mesozoic-Cenozoic evolution of North American Cordilleran MCCs.

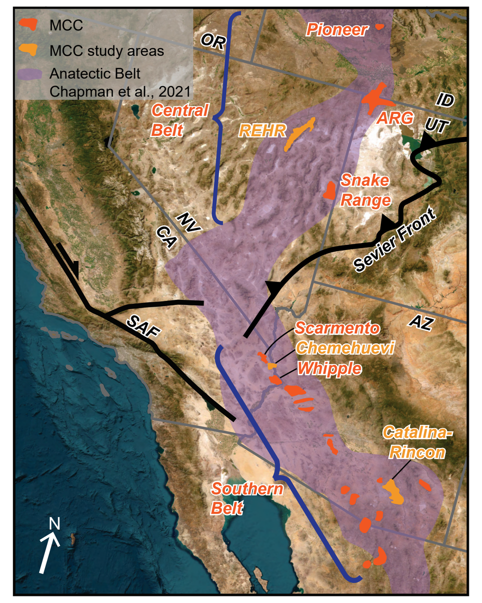

Endmember models of MCC generation

Extension-driven MCC: Shear zone as the down-dip continuation of detachment

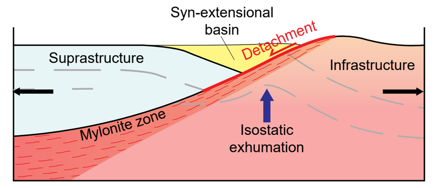

- Large-magnitude regional extension (>~100% extension; Wernicke, 1981; Davis, 1983) is accommodated by detachment faulting and its down-dip continuation of ductile shearing
- Mylonitic shear zone **shares the same kinematics and is coeval** with detachment fault (Wernicke, 1981; Davis, 1983)
- Hanging wall removal leads to **isostatic exhumation** (Wernicke and Axen, 1988 *Geology*)
- Hanging wall receives **syn-kinematic sediments** from the unroofing footwall (Yin and Dunn, 1992 *GSAB*)**

Extension-driven MCC: Detachment fault captures mid-crust shear zone

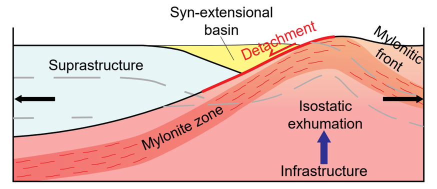

- Detachment captures preexisting mid-crustal shear zone (e.g., mylonitic front; Davis, 1988 *Geologische Rundschau*)
- Mylonitic fabrics at the mylonitic front departs away from the detachment
- Mylonitic shear zone is **kinematically decoupled** from the detachment
- Timing of mylonitic shearing can be **coeval or older** than detachment faulting

Buoyant diapir MCC: Detachment fault captures a diapiric shear zone

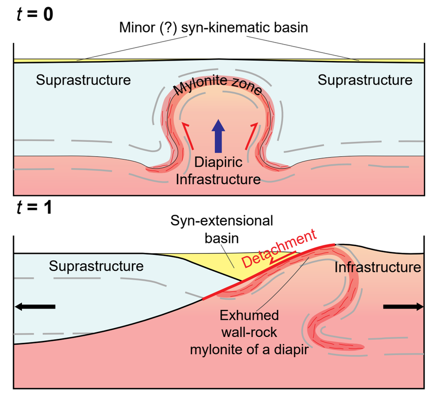

- Crustal heating and melting drives density instability, and emplacement of a buoyant diapir in the mid-crust (t = 0; Konstantinou et al., 2012 *Geosphere*)
- Charaterized by **syn-diapir leucrogranite intrusion** and **primarily pure-shear strain** at the wall-rock shear zone (Zuza et al., 2024 *EPSL*)
- **Minor (?) syn-diapir sedimentation** due to dynamic topography (t = 0)
- Detachment fault exhumes the preexisting mid-crust diapir to the surface
- Requires wall-rock mylonite to **predate** detachment faulting

EBSD microstructure

- **Crystallographic vorticity axis** (CVA; Michels et al., 2015) calculates the rotational axis when the rock is under shear
- Identical CVAs between accessory phases (e.g., apatite, titanite) and fabric-forming phases (e.g., quartz) suggest they share the same deformation kinematics (Miranda et al., 2023 *Geology*)

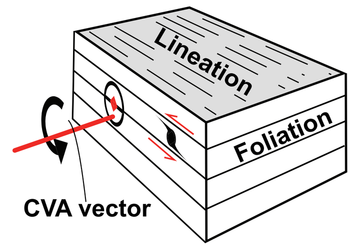

Modified from Michels et al. (2015 *Geology*)

Key for the low-angle boundary (LAB) misorientation analysis

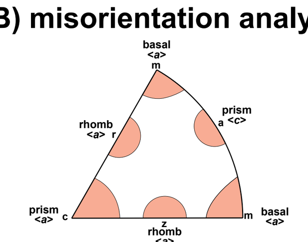

Modified from Neumann (2000 *Journal of Structural Geology*)

REHR

- Proterozoic–Paleozoic sedimentary rocks are metamorphosed and intruded by Jurassic–Oligocene leucogranite (Howard et al., 2011 *Geosphere*)
- West-flank is bounded by the late-Oligocene NW-directed mylonitic shear zone (Snoke, 1980 *GSA Memoirs*)
- Brittle normal-sense faulting initiated during mid-Miocene (Colgan et al., 2010 *Tectonics*)
- Infrastructure records possible Jurassic–Cretaceous contractional deformation (Hudec, 1992; McGrew et al., 2000 *GSAB*)
- Ongoing mapping at the transition zone (blue box) between the metamorphosed infrastructure and brittle suprastructure in the central Ruby Mountains

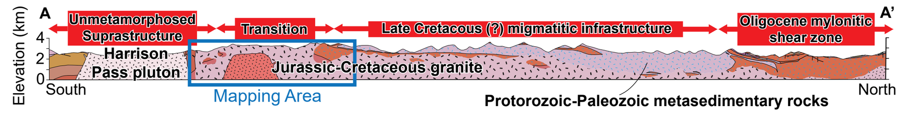

Modified from Howard et al. (1979 *USGS*)

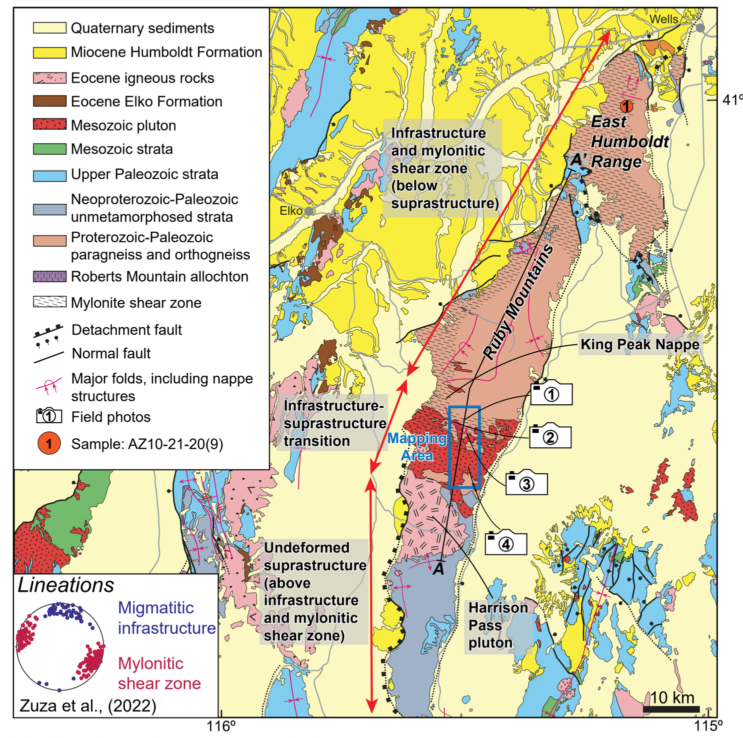

Modified from Colgan et al. (2010)

Field observations of the infrastructure-suprastructure transition

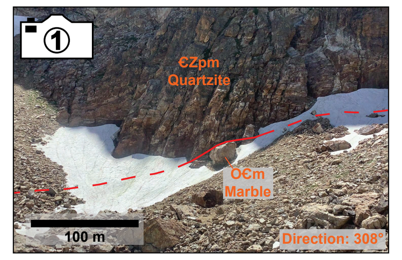

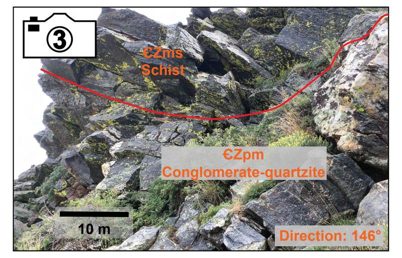

Photo 1: Inverted stratigraphy with Cambrian–Proterozoic Prospect Mountains quartzite (ЄZpm) overlays on top of Cambrain–Ordovician marble (OЄm).

Photo 3: Inverted stratigraphy with Cambrain–Proterozoic McCoy Creek schist (ЄZms) overlays ЄZpm.

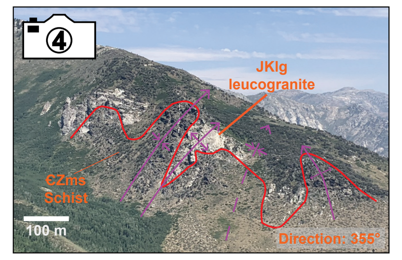

Photo 2: Weakly foliated and folded ЄZpm at the upper limb of King Peak nappe.

Photo 4: Upright, north-plunging fold train between Jurassic–Cretaceous leucogranite (JKlg) and ЄZms near the suprastructure transition.

Preliminary apatite U-Pb ages, microstructure, and zircon U-Pb geochronology

AZ10-21-20(9): Monzogranite

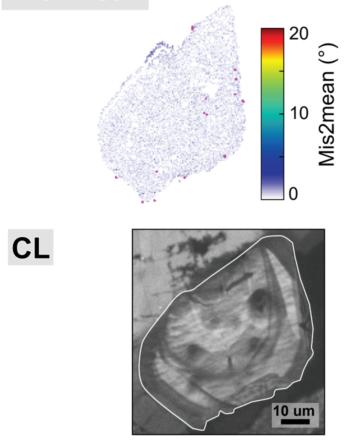

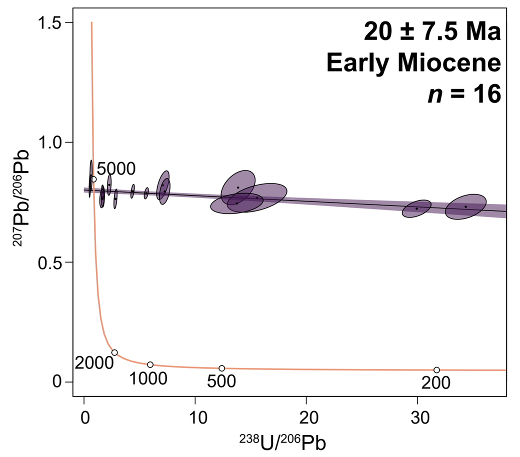

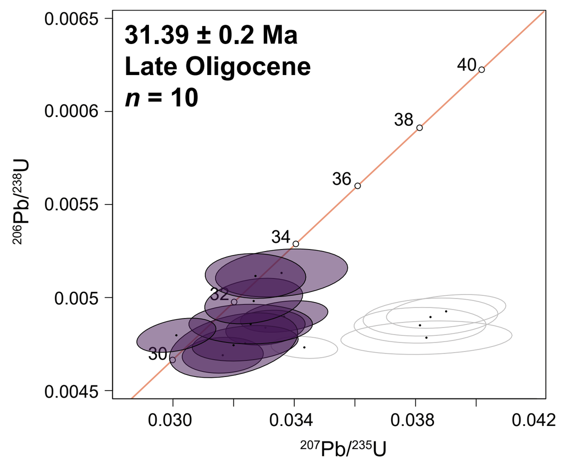

- **Apatite U-Pb ages yield Early Miocene ages**, which is **similar to the $^{40}Ar/^{39}Ar$ mica dates** in the northern Ruby Mountains (Dallmeyer et al., 1986 Tectonics)
- Apatite U-Pb ages likely represent **thermochronologic dates** (Apatite $T_c \approx$ 350-570°C; Chew and Sikings, 2021 *Minerals*)
- **Zircon U-Pb ages yield late Oligocene crystallization ages**, consistent with extensive leucogranite intrusions in REHR

Summary

- **Inverted contacts support km-scale recumbent folding in the central Ruby Mountains**, but prelimianry field observations suggest that **equivalent units are less strained compared to the northern Ruby Mountains-East Humboldt Range**
- Zircon U-Pb geochronology will be conducted for the central Ruby Mountains leucrogranite complex in Fall 2024 to understand the intrusion history and to constrain the deformation timing at the transition zone
- **Undeformed apatite U-Pb ages are consistent with existing Early Miocene $^{40}Ar/^{39}Ar$ mica cooling dates, thus we intrepret it as a thermochronologic date**

Chemehuevi

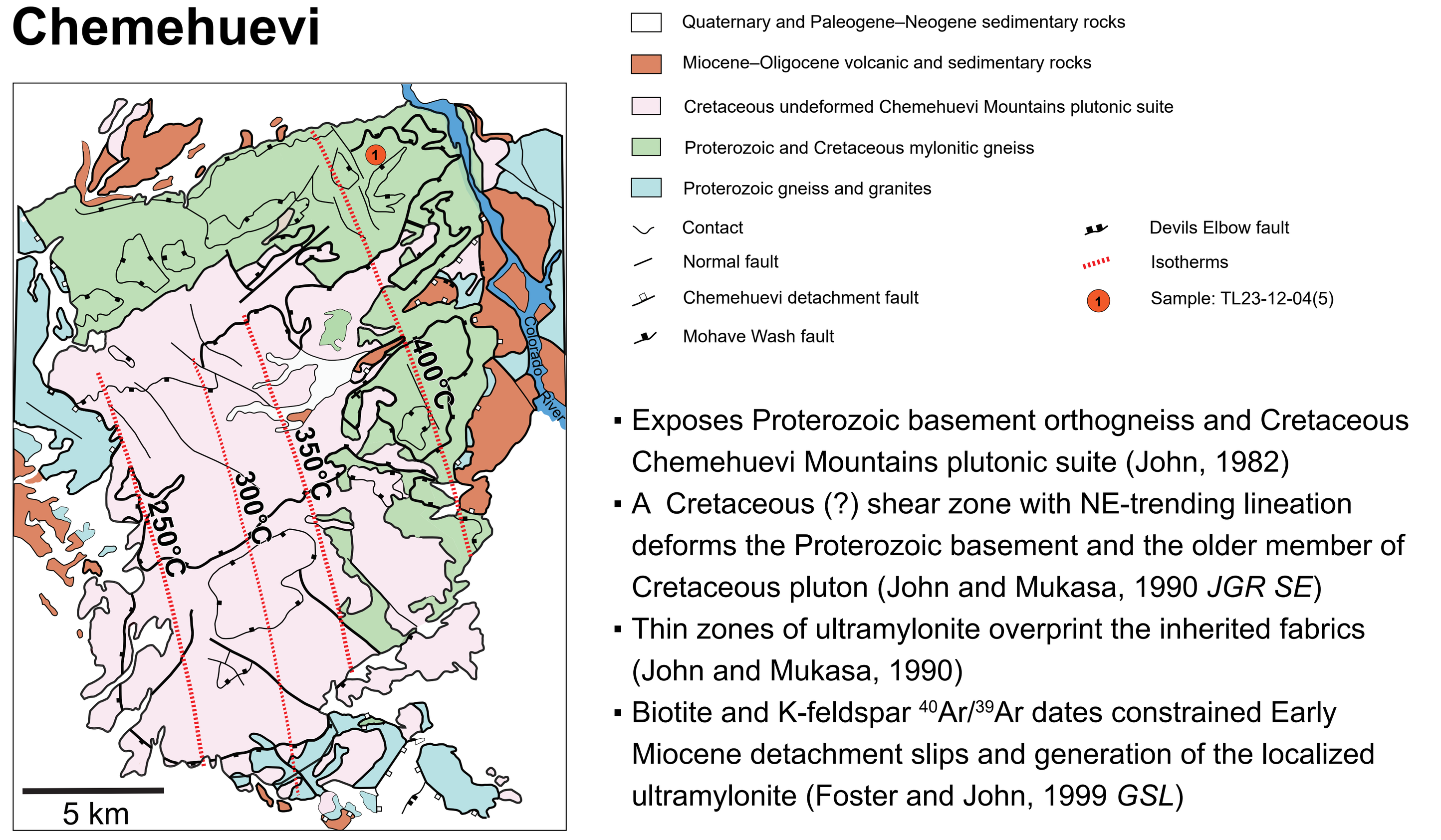

Modified from LaForge et al. (2017 *Geosphere*)

- Exposes Proterozoic basement orthogneiss and Cretaceous Chemehuevi Mountains plutonic suite (John, 1982)
- A Cretaceous (?) shear zone with NE-trending lineation deforms the Proterozoic basement and the older member of Cretaceous pluton (John and Mukasa, 1990 *JGR SE*)
- Thin zones of ultramylonite overprint the inherited fabrics (John and Mukasa, 1990)
- Biotite and K-feldspar $^{40}Ar/^{39}Ar$ dates constrained Early Miocene detachment slips and generation of the localized ultramylonite (Foster and John, 1999 *GSL*)

Preliminary microstructure and apatite U-Pb petrochronology

TL23-12-04(5): Garnet-biotite orthogneiss

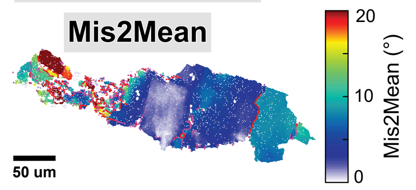

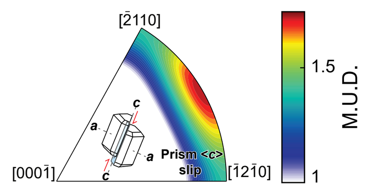

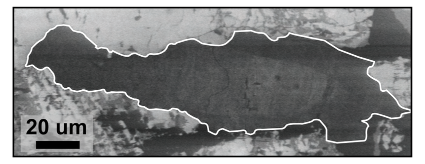

- Misorientation map exhibits apatite grain size reduction and intragrain deformation
- Low-angle boundary (LAB) misorientation axis indicates dislocation around <*a*> axis, inferring prism <*c*> slip

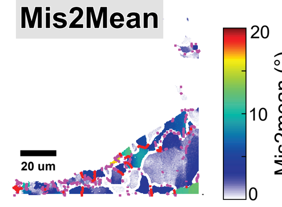

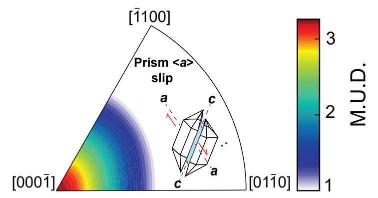

- LAB misorientation axis suggests dislocation arrays around <*c*> axis, implying deformation mechanism dominated by **prism <*a*> slip**
- Prism <*a*> slip in quartz suggests deformation condition at **~500°C**

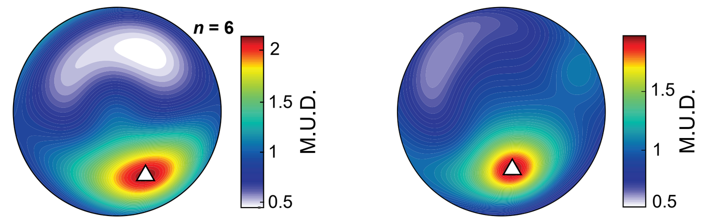

- **Quartz CVA vector is subparallel to the mean apatite CVA**, signifying that they share **identical deformation kinematics**

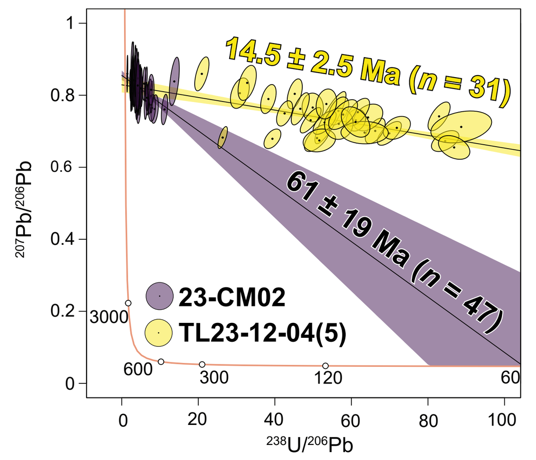

Summary

- New EBSD mircrostructure constrains the **mylonitization temperature to ~500°C** (prism <*a*> slip in quartz)
- **New apatite U-Pb petrochronology yields Late Cretaceous and middle Micoene ages**
- Middle Miocene apatite U-Pb ages is slightly younger than the $^{40}Ar/^{39}Ar$ biotite cooling dates at ~20 Ma (Foster and John, 1999)
- **Our apatite U-Pb age populations record the timing of both Late Cretaceous ductile (contractional) shearing and Miocene ultramylonite formation**

Catalina-Rincon

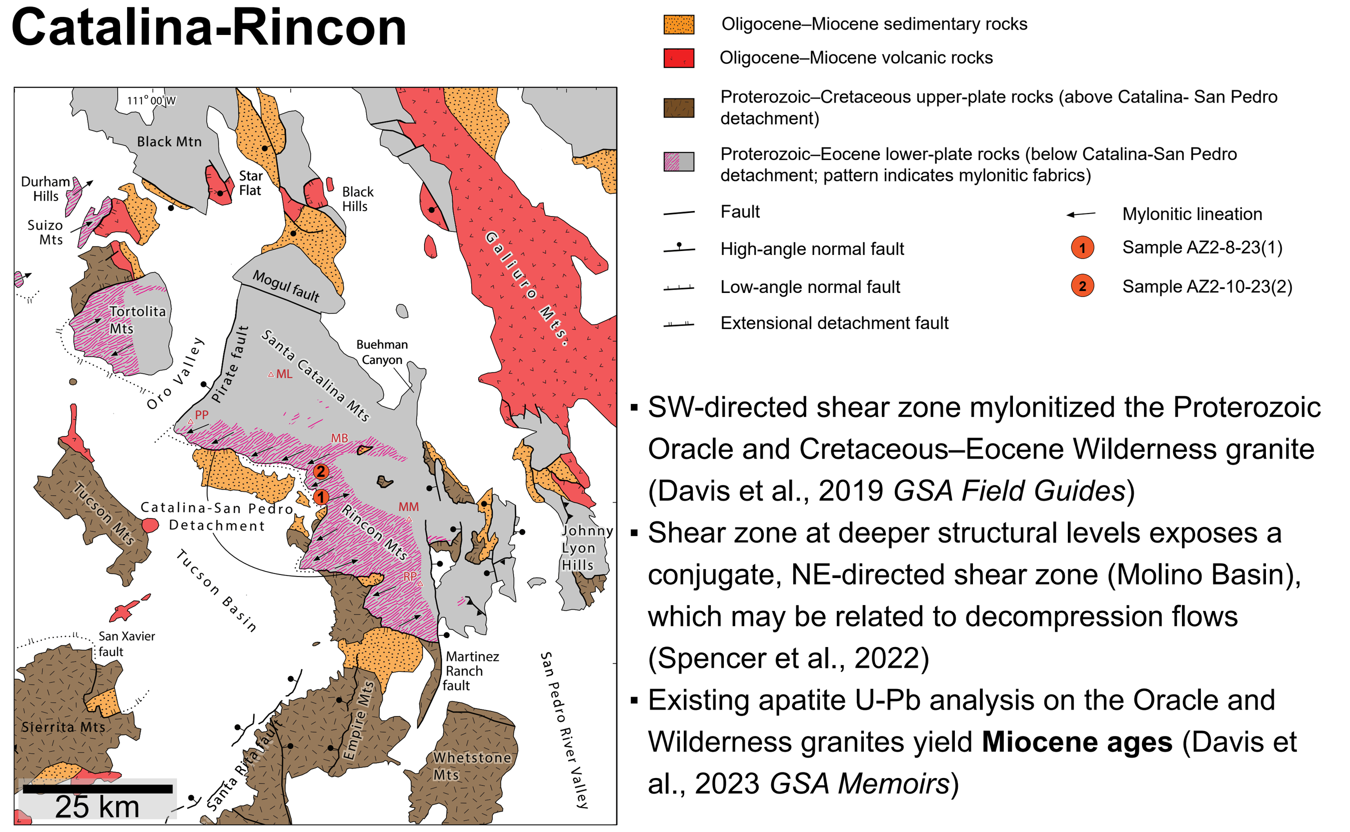

Modified from Spencer et al. (2022 *Geosphere*)

- SW-directed shear zone mylonitized the Proterozoic Oracle and Cretaceous–Eocene Wilderness granite (Davis et al., 2019 *GSA Field Guides*)
- Shear zone at deeper structural levels exposes a conjugate, NE-directed shear zone (Molino Basin), which may be related to decompression flows (Spencer et al., 2022)
- Existing apatite U-Pb analysis on the Oracle and Wilderness granites yield **Miocene ages** (Davis et al., 2023 *GSA Memoirs*)

Preliminary microstructure

AZ2-8-23(1): Mylonitic Oracle granite

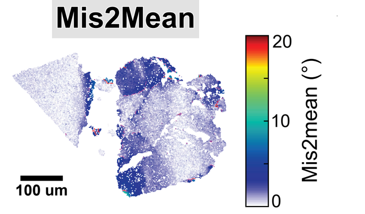

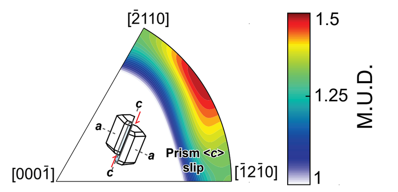

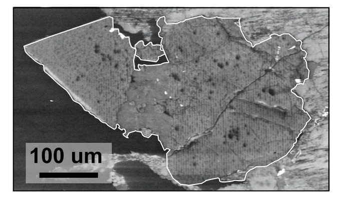

- Dislocation on apatite with LAB misorientation axis around <a> axis, suggests **prism <c> slip**
- Homogenous CL texture

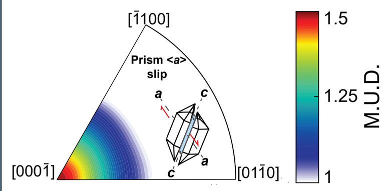

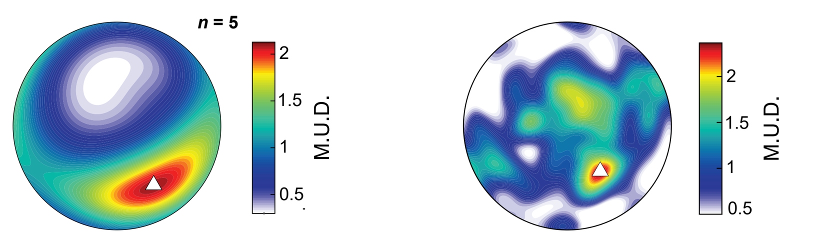

- Deformed quartz with prism <*a*> slip, suggests deformation temeprature at ~500°C
- **Subparalle CVAs between apatite and quartz**, thus they share the same deformation kinematics

Preliminary apatite U-Pb petrochronology

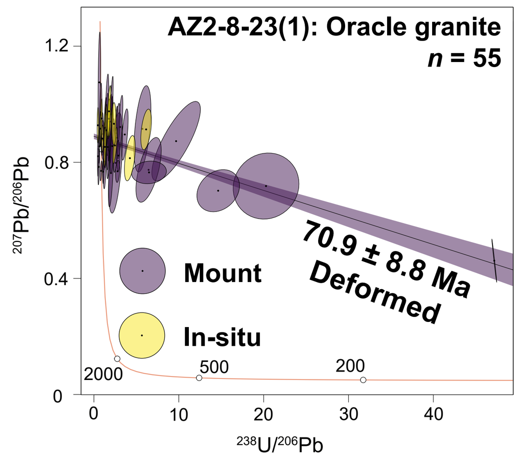

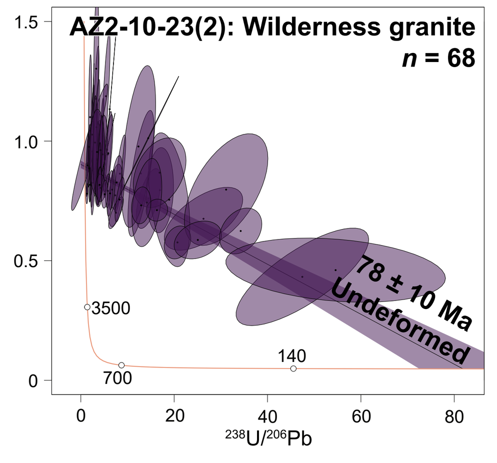

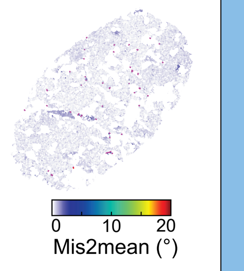

Summary

- Deformed apatite from the Oracle-type granite and undeformed apatite from the Wilderness-type granite consistently yields late Cretaceous U-Pb ages
- **Inconsistent with the existing Miocene ages from the Rincon Mountains** (Davis et al., 2023)
- **Do the new Cretaceous ages record the timing of Mesozoic contractional deformation?**